Supporting Information For

Adhesion behaviour of bulk supramolecular polymers via pillar[5]arene-based molecular recognition

Jinlei Lai[a], Shiyu Huang[a], Shuanggen Wu[a], Fenfang Li[b], Shengyi Dong*[a]

[a]College of Chemistry and Chemical Engineering, Hunan University, Changsha 410082, Hunan (P. R. China).

E-mail: dongsy@hnu.edu.cn

[b]College of Chemistry and Chemical Engineering, Central South University, Changsha 410083, Hunan (P. R. China).

1. Materials and Methods

All acids were commercially available. **WP5** was synthesized according to previously reported procedures.[S1,S2] Supramolecular polymers were prepared according to the previous literatures.[S3,S4] ^{1}H NMR spectra were collected on a Bruker-AV400. Two-dimensional NOESY experiments were collected on a Bruker-AV400. Fourier-transform IR (FT-IR) spectra were recorded on SHIMADZU QATR-S. Scanning electron microscopy (SEM) images were performed on a JEOL JSM-7610F. Powder X-Ray Diffraction (PXRD) data was collected on a Bruker D8 ADVANCE. Differential Scanning Calorimeter (DSC) measurements were carried out using TAQ100 from -60 to 100 °C with a heating rate of 10 °C min^{-1} under nitrogen atmosphere. Thermogravimetric analysis (TGA) was carried out using a TGA5500, the heating rate was 10 °C min^{-1} from 30 to 600 °C in nitrogen atmosphere. Rheology measurements were collected on an Anton Paar MCR 92. The adhesion strength measurements were performed on a HY-0580 Electronic tensile testing machine. The conductivity of solution was collected on a DDSJ-308F. The bulk resistivity was carried out using a ST2643. Powder resistivity was collected on a ST2722 resistivity of the powder tester.

Experimental Section

Preparation of adhesion layers: pillar[5]arene-based supramolecular adhesives were coated on the surface of a plate (glass, steel, PMMA, PTFE), then a new plate was covered on the adhesive layer. After pressing and heating for 30 min, a thin coating layer was formed and two surfaces were adhered firmly.

Temperature- or RH-dependent adhesion tests: The adhered plates were stored at different temperatures or relative humidity for three hours before lap-shear tests.

2. Supramolecular Adhesives Preparation and Characterization

All pillar[5]arene-based supramolecular adhesives were synthesized according to present literatures.[S1,S2] By simply heating the aqueous solution **WP5** and acids with different molar ratios at 70 °C, pillar[5]arene-based bulk supramolecular polymer materials were obtained. For example, water-soluble pillar[5]arene **WP5** (2.6 g, 1.1 mmol) and DL-tartaric acid (1.7g, 11 mmol) were added into a 100 mL beaker, and then 15 mL of water was added. **PD-2** was obtained after heating the mixture solution for 12 h at 70 °C. With the evaporation of water, the aqueous solution was converted to transparent and highly viscous bulk supramolecular adhesives.

Table S1. Pillar[5]arene-based supramolecular adhesives.

Number	WP5 : Acids	Molar ratio	Abbreviation
1	**WP5** : Tetrahydrofuran-2,3,4,5-tetracarboxylic acid	1 : 5	**PT-1**
2	**WP5** : Tetrahydrofuran-2,3,4,5-tetracarboxylic acid	1 : 10	**PT-2**
3	**WP5** : Tetrahydrofuran-2,3,4,5-tetracarboxylic acid	1 : 20	**Solid**
4	**WP5** : Citric acid	1 : 5	**PC-1**
5	**WP5** : Citric acid	1 : 10	**PC-2**
6	**WP5** : Citric acid	1 : 20	**PC-3**
7	**WP5** : DL-Tartaric acid	1 : 5	**PD-1**
8	**WP5** : DL-Tartaric acid	1 : 10	**PD-2**
9	**WP5** : DL-Tartaric acid	1 : 20	**Solid**

3. Macroscopic Pictures of Supramolecular Adhesives

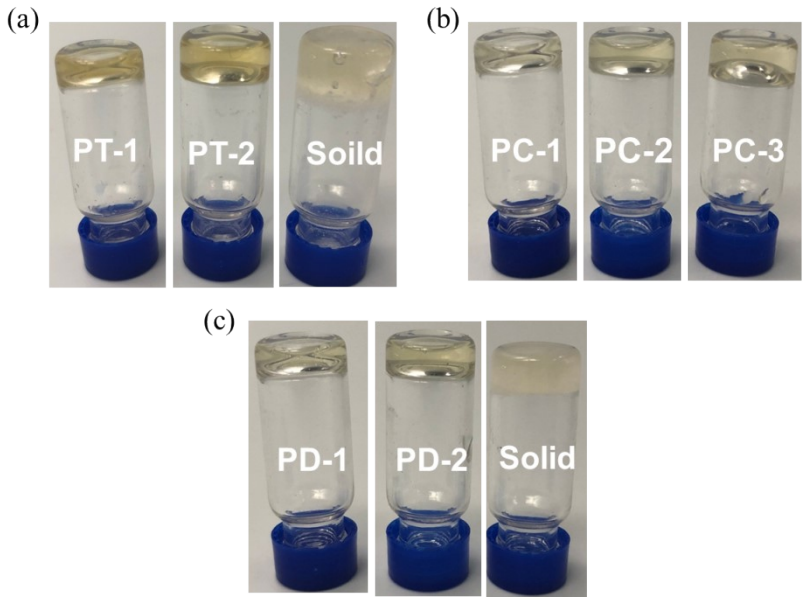

Fig. S1 WP5-based supramolecular adhesives with different molar ratios: (a) tetrahydrofuran-2,3,4,5-tetracarboxylic acid; (b) citric acid; (c) DL-tartaric acid.

4. *^{1}H NMR Spectra of Supramolecular Adhesives*

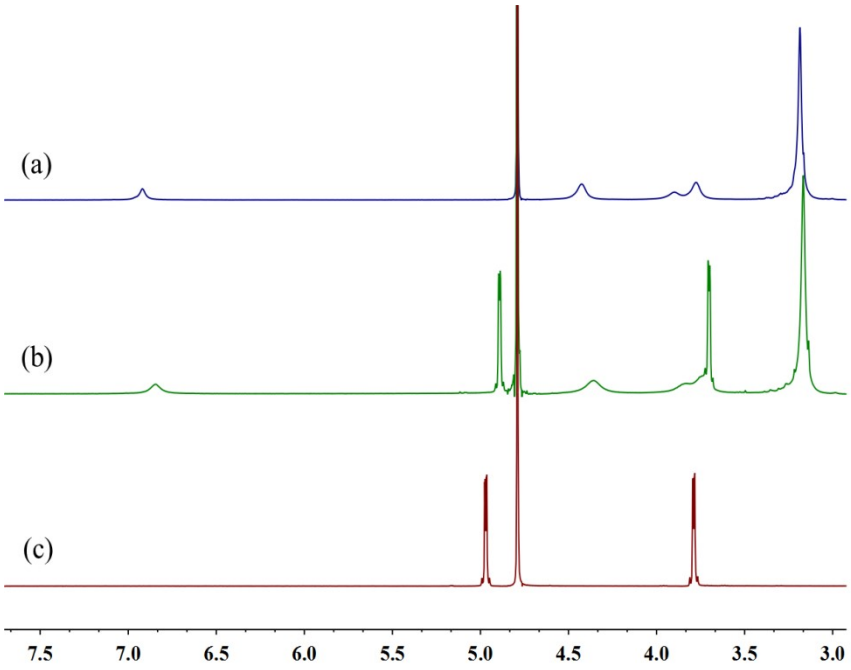

Fig. S2 Partial ^{1}H NMR spectra (400 MHz, D_2O, 25 °C): (a) **WP5** (5.2×10^{-3} M); (b) **PT-2** (5.2×10^{-3} M); (c) tetrahydrofuran-2,3,4,5-tetracarboxylic acid (5.2×10^{-2} M).

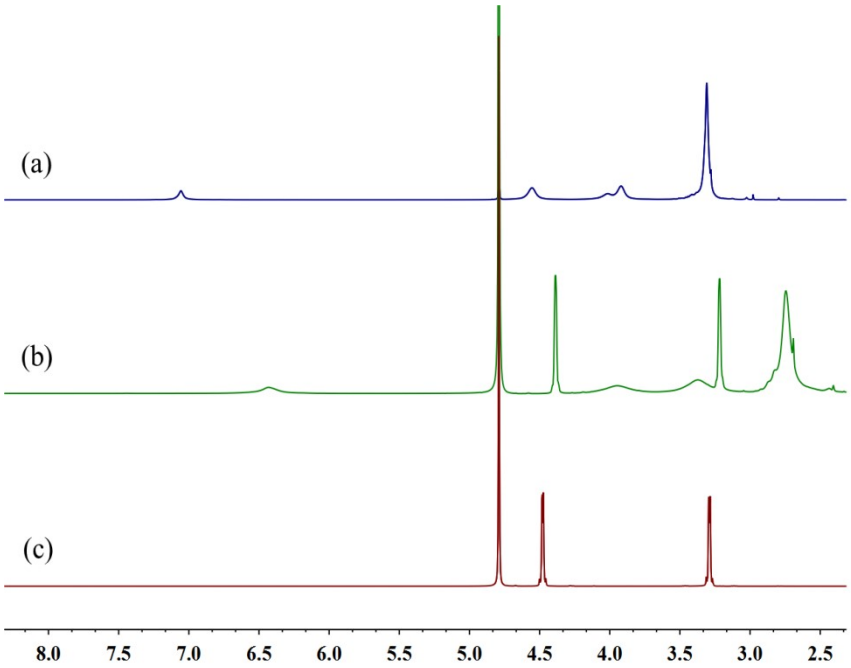

Fig. S3 Partial ^{1}H NMR spectra (400 MHz, D_2O, 25 °C): (a) **WP5** (1.7×10^{-1} M); (b) **PT-2** (1.7×10^{-1} M); (c) tetrahydrofuran-2,3,4,5-tetracarboxylic acid (1.7 M).

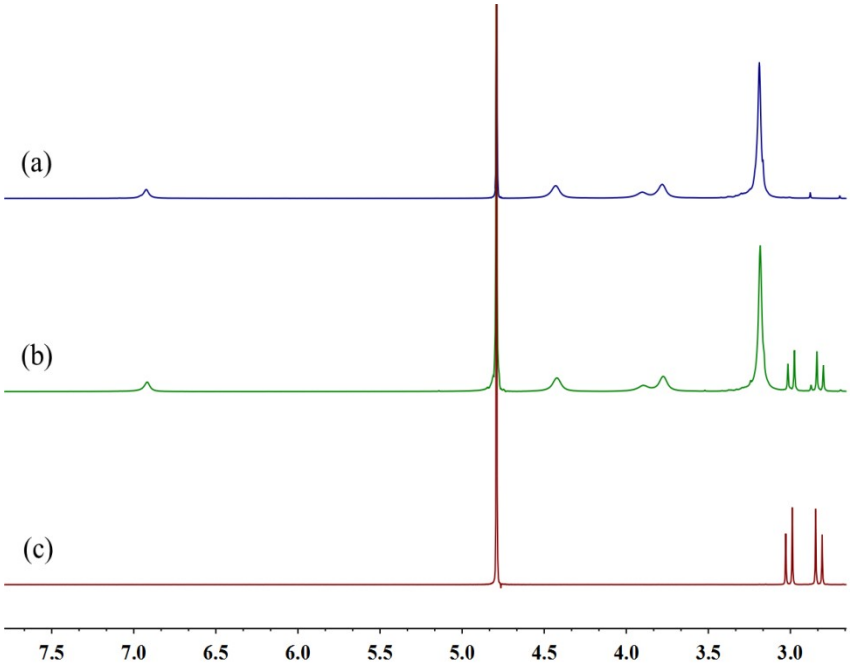

Fig. S4 Partial ^{1}H NMR spectra (400 MHz, D_2O, 25 °C): (a) **WP5** (7.8×10^{-3} M); (b) **PC-1** (7.8×10^{-3} M); (c) citric acid (3.9×10^{-2} M).

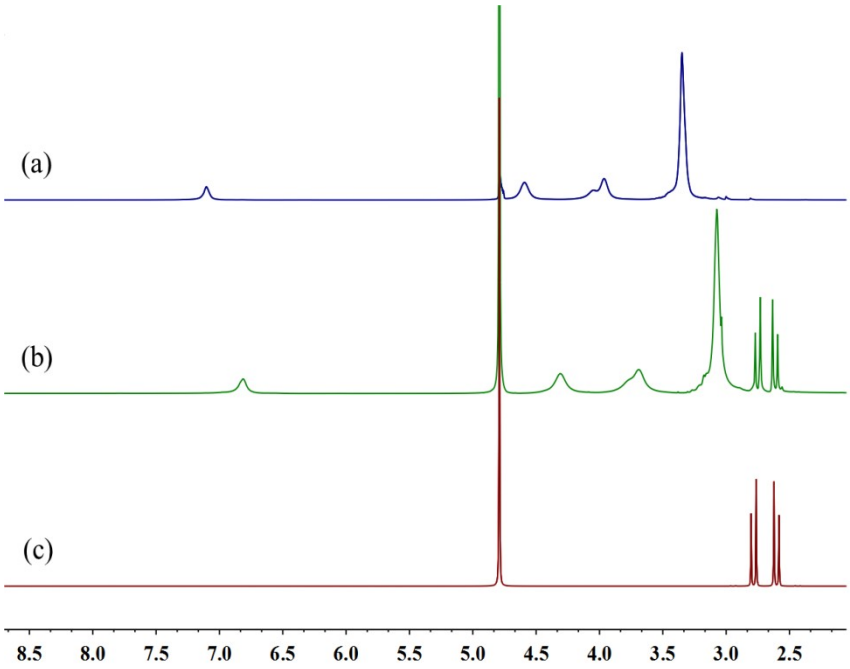

Fig. S5 Partial ^{1}H NMR spectra (400 MHz, D_2O, 25 °C): (a) **WP5** (2.5×10^{-1} M); (b) **PC-1** (2.5×10^{-1} M); (c) citric acid (1.25 M).

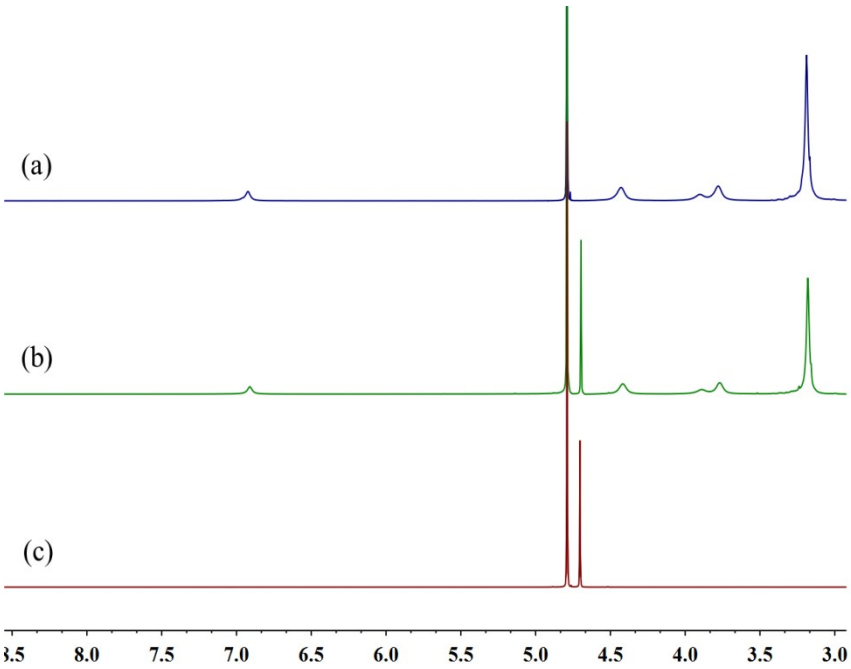

Fig. S6 Partial ^{1}H NMR spectra (400 MHz, D_2O, 25 °C): (a) **WP5** (6.6×10^{-3} M); (b) **PD-2** (6.6×10^{-3} M); (c) DL-tartaric acid (6.6×10^{-2} M).

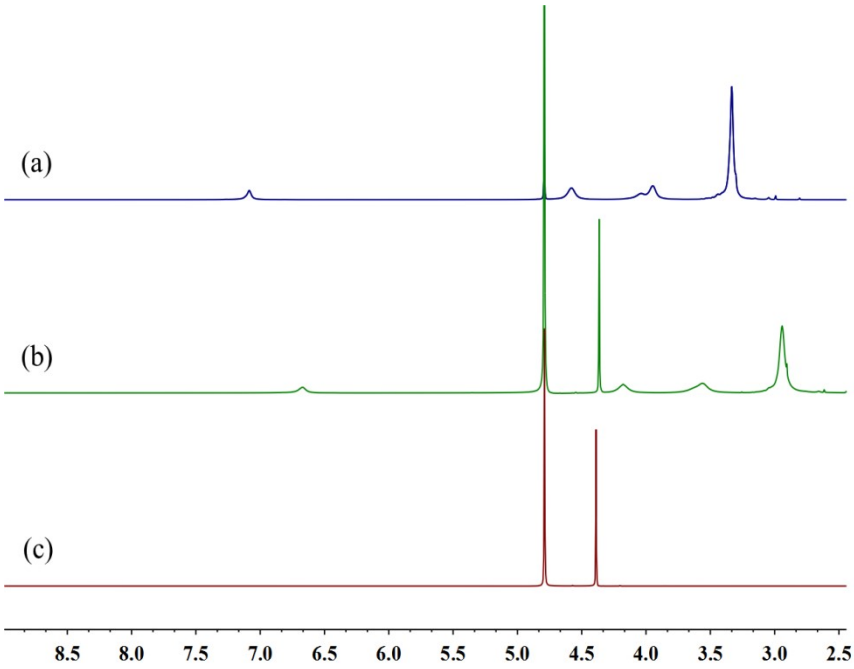

Fig. S7 Partial ^{1}H NMR spectra (400 MHz, D_2O, 25 °C): (a) **WP5** (2.1×10^{-1} M); (b) **PD-2** (2.1×10^{-1} M); (c) DL-tartaric acid (2.1 M).

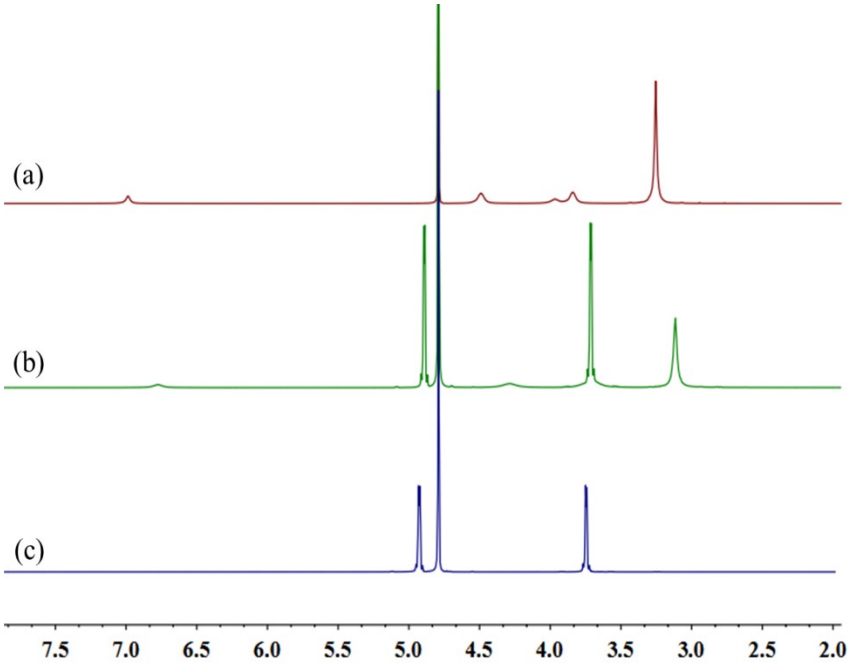

Fig. S8 Partial ^{1}H NMR spectra (400 MHz, D_2O, 25 °C): (a) **WP5** (1.0×10^{-2} M); (b) a mixture of **WP5** and tetrahydrofuran-2,3,4,5-tetracarboxylic acid (molar ratio = 1:40, 1.0×10^{-2} M) without heating ; (c) tetrahydrofuran-2,3,4,5-tetracarboxylic acid (0.4 M).

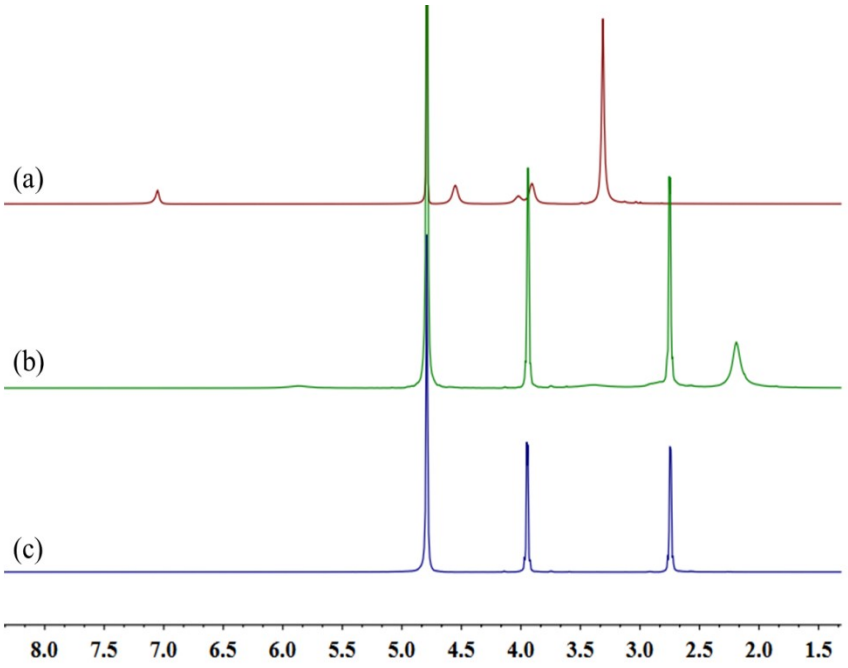

Fig. S9 Partial ^{1}H NMR spectra (400 MHz, D_2O, 25 °C): (a) **WP5** (0.1 M); (b) a mixture of **WP5** and tetrahydrofuran-2,3,4,5-tetracarboxylic acid (molar ratio = 1:40, 0.1 M) without heating; (c) tetrahydrofuran-2,3,4,5-tetracarboxylic acid (4 M).

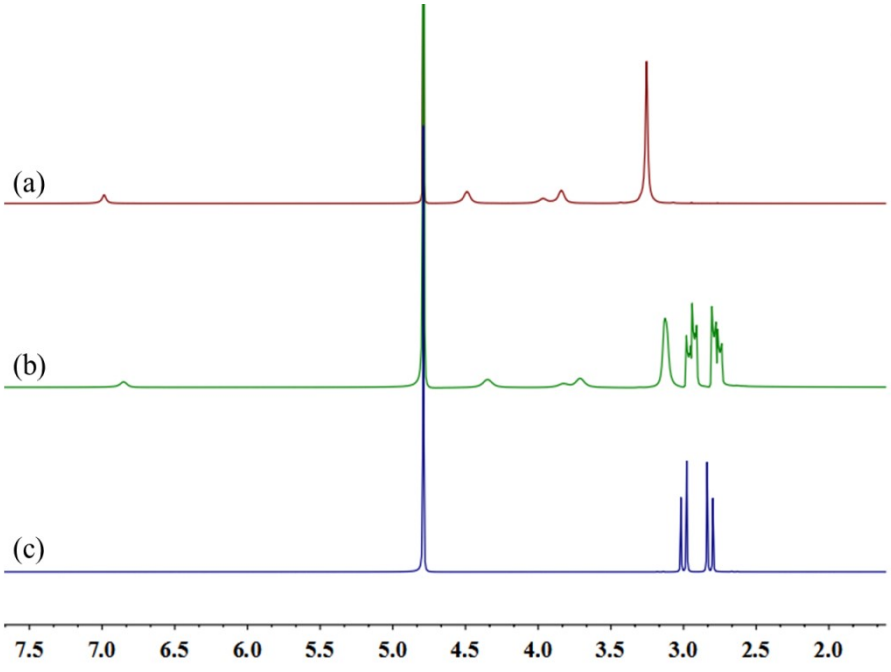

Fig. S10 Partial ^{1}H NMR spectra (400 MHz, D_2O, 25 °C): (a) **WP5** (1.0×10^{-2} M); (b) a mixture of **WP5** and citric acid (molar ratio = 1:40, 1.0×10^{-2} M) without heating; (c) citric acid (0.4 M).

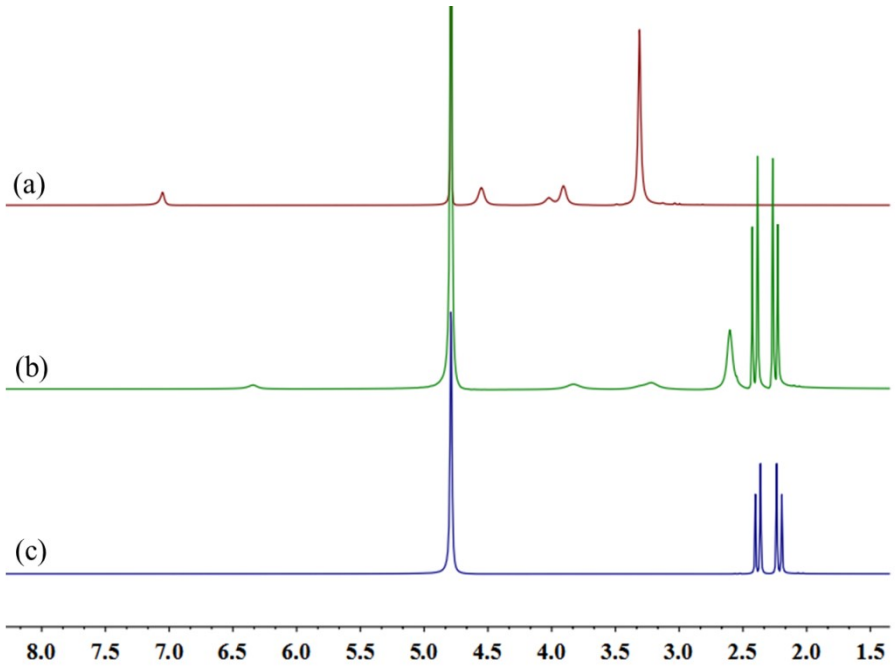

Fig. S11 Partial ^{1}H NMR spectra (400 MHz, D_2O, 25 °C): (a) **WP5** (0.1 M); (b) a mixture of **WP5** and citric acid (molar ratio = 1:40, 0.1 M) without heating; (c) citric acid (4 M).

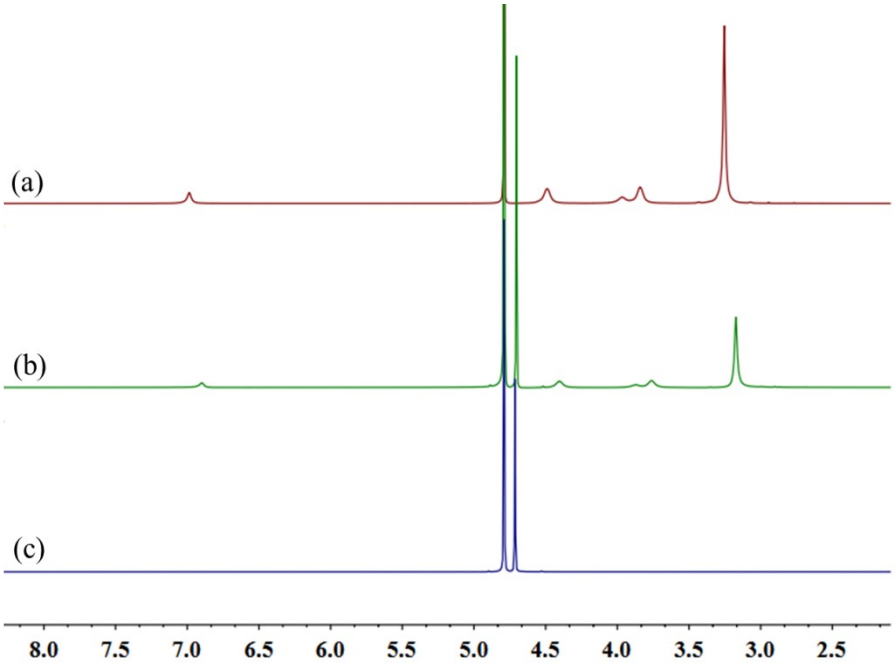

Fig. S12 Partial ^{1}H NMR spectra (400 MHz, D_2O, 25 °C): (a) **WP5** (1.0×10^{-2} M); (b) a mixture of **WP5** and DL-tartaric acid (molar ratio = 1:40, 1.0×10^{-2} M) without heating; (c) DL-tartaric acid (0.4 M).

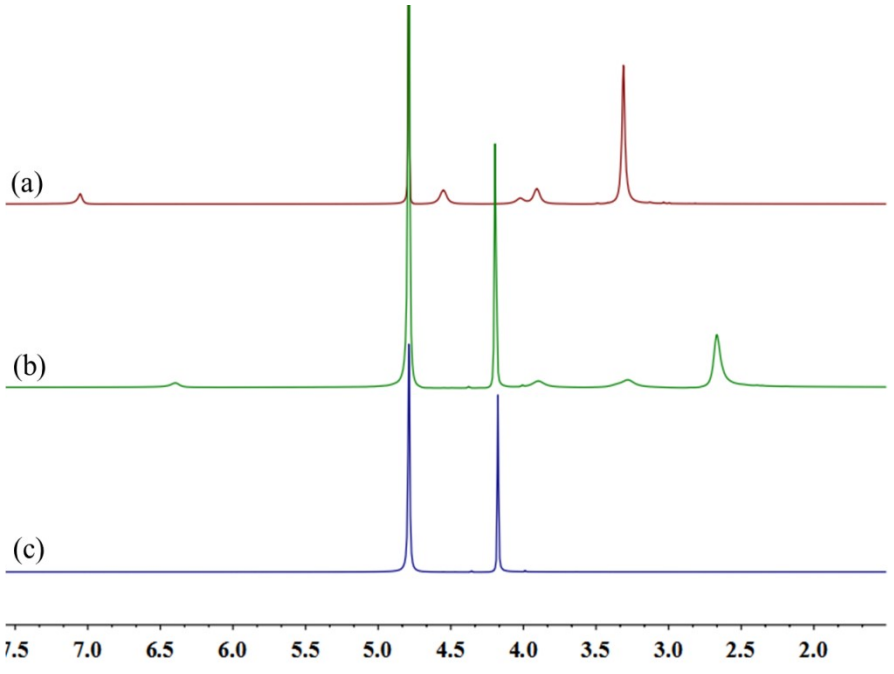

Fig. S13 Partial ^{1}H NMR spectra (400 MHz, D_2O, 25 °C): (a) **WP5** (0.1 M); (b) a mixture of **WP5** and DL-tartaric acid (molar ratio = 1:40, 0.1 M) without heating; (c) DL-tartaric acid (4 M).

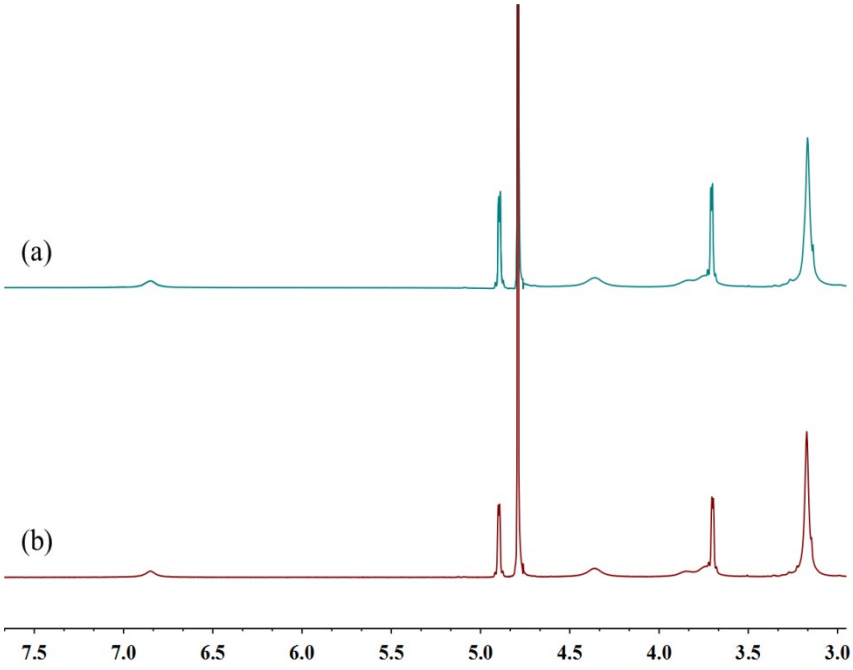

Fig. S14 Partial ^{1}H NMR spectra (400 MHz, D_2O, 25 °C): (a) a mixture of **WP5** and tetrahydrofuran-2,3,4,5-tetracarboxylic acid (molar ratio = 1:10, 25 mg mL^{-1}) without heating; (b) **PT-2** (25 mg mL^{-1}).

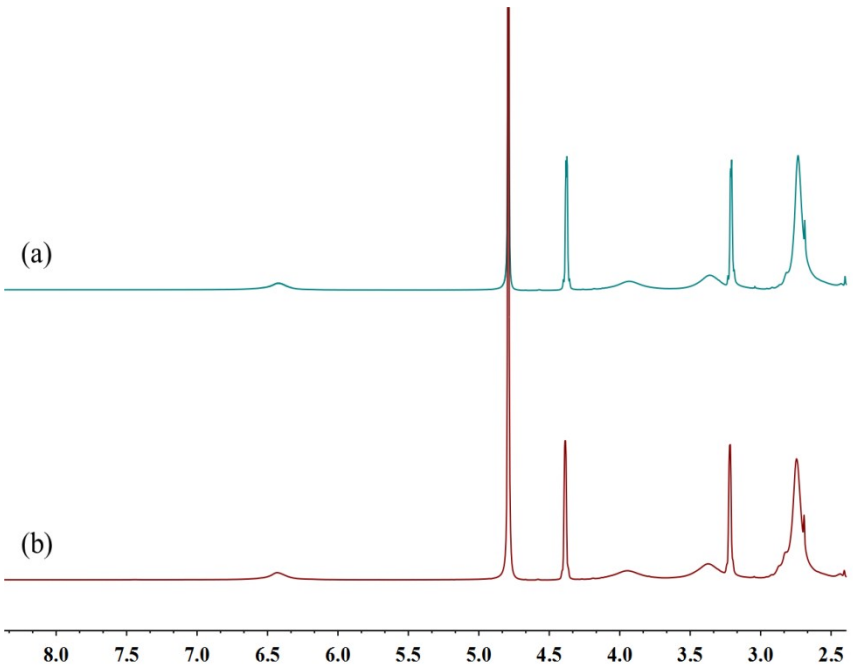

Fig. S15 Partial ^{1}H NMR spectra (400 MHz, D_2O, 25 °C): (a) a mixture of **WP5** and tetrahydrofuran-2,3,4,5-tetracarboxylic acid (molar ratio = 1:10, 800 mg mL^{-1}) without heating; (b) **PT-2** (800 mg mL^{-1}).

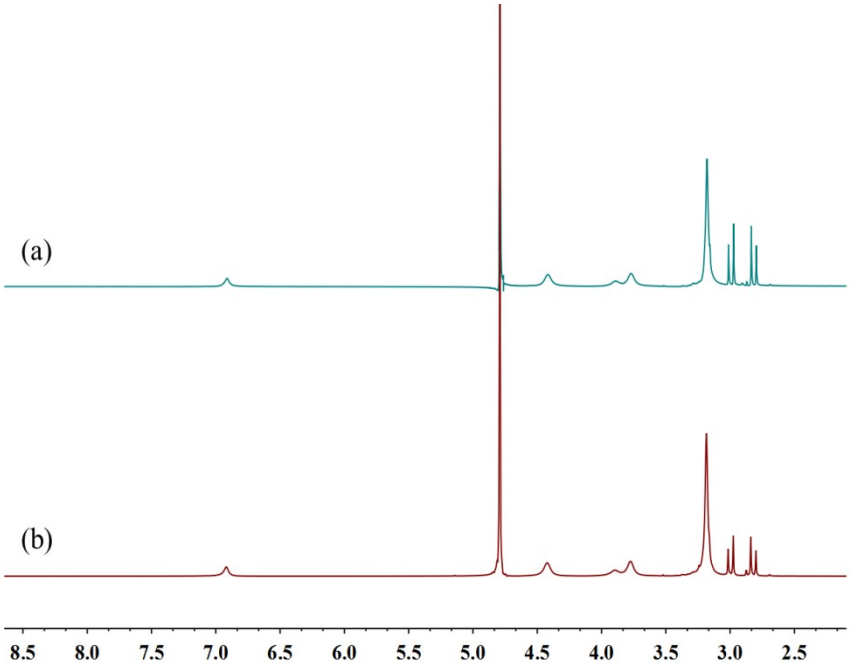

Fig. S16 Partial ^{1}H NMR spectra (400 MHz, D_2O, 25 °C): (a) a mixture of **WP5** and citric acid (molar ratio = 1:5, 25 mg mL^{-1}) without heating; (b) **PC-1** (25 mg mL^{-1}).

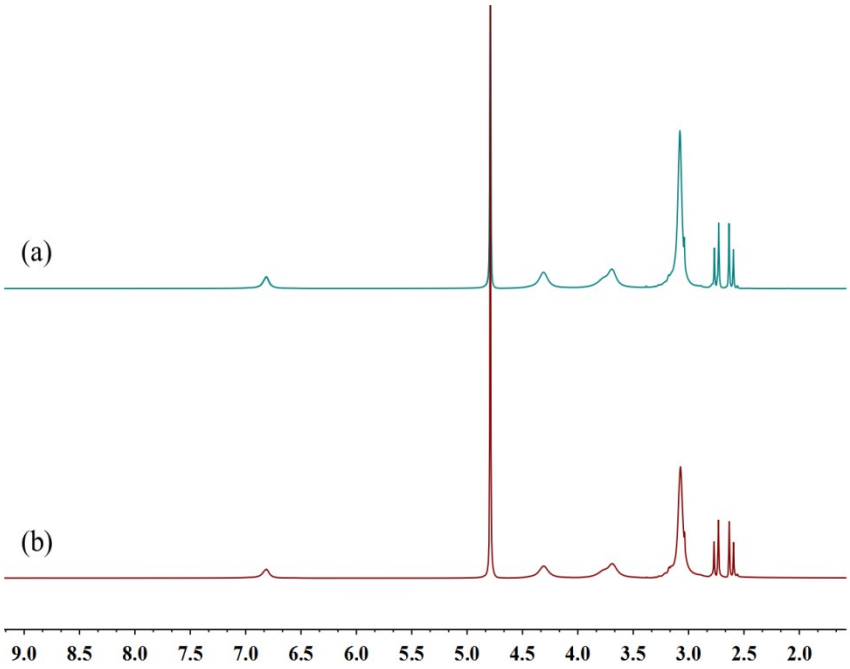

Fig. S17 Partial ^{1}H NMR spectra (400 MHz, D_2O, 25 °C): (a) a mixture of **WP5** and citric acid (molar ratio = 1:5, 800 mg mL^{-1}) without heating; (b) **PC-1** (800 mg mL^{-1}).

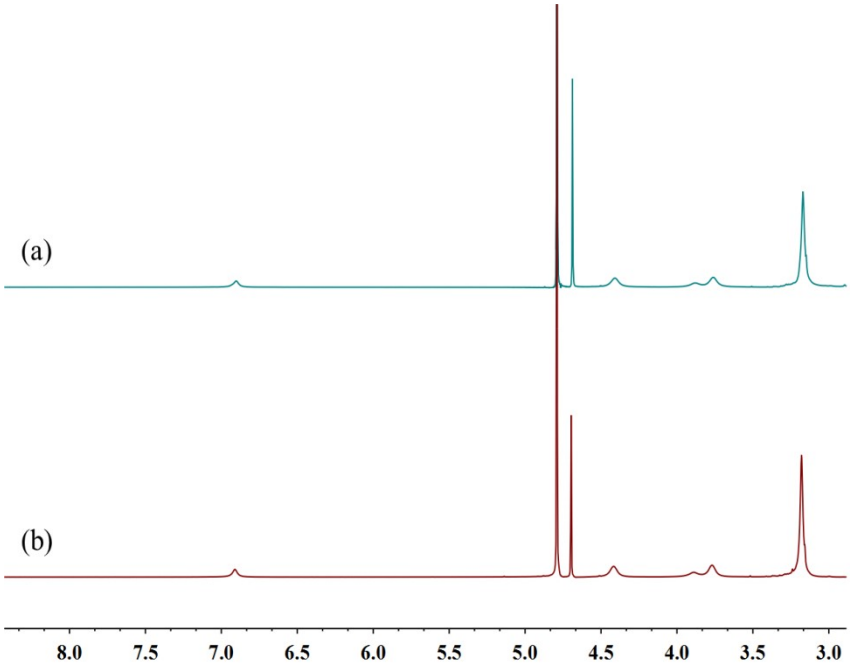

Fig. S18 Partial ^{1}H NMR spectra (400 MHz, D_2O, 25 °C): (a) a mixture of **WP5** and DL-tartaric acid (molar ratio = 1:10, 25 mg mL^{-1}) without heating; (b) **PD-2** (25 mg mL^{-1}).

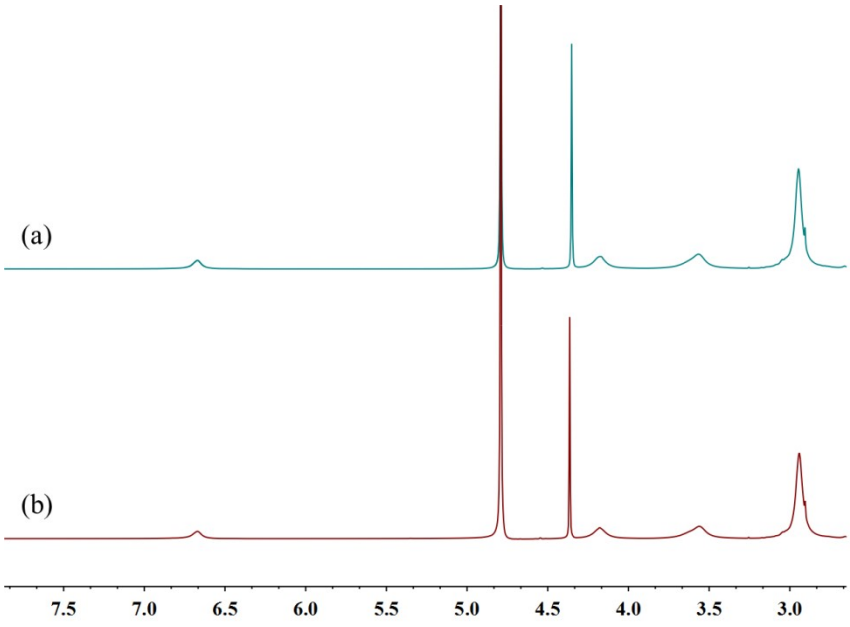

Fig. S19 Partial ^{1}H NMR spectra (400 MHz, D_2O, 25 °C): (a) a mixture of **WP5** and DL-tartaric acid (molar ratio = 1:10, 800 mg mL^{-1}) without heating; (b) **PD-2** (800 mg mL^{-1}).

5. *Concentration-Dependent ^{1}H NMR Spectra of Supramolecular Adhesives*

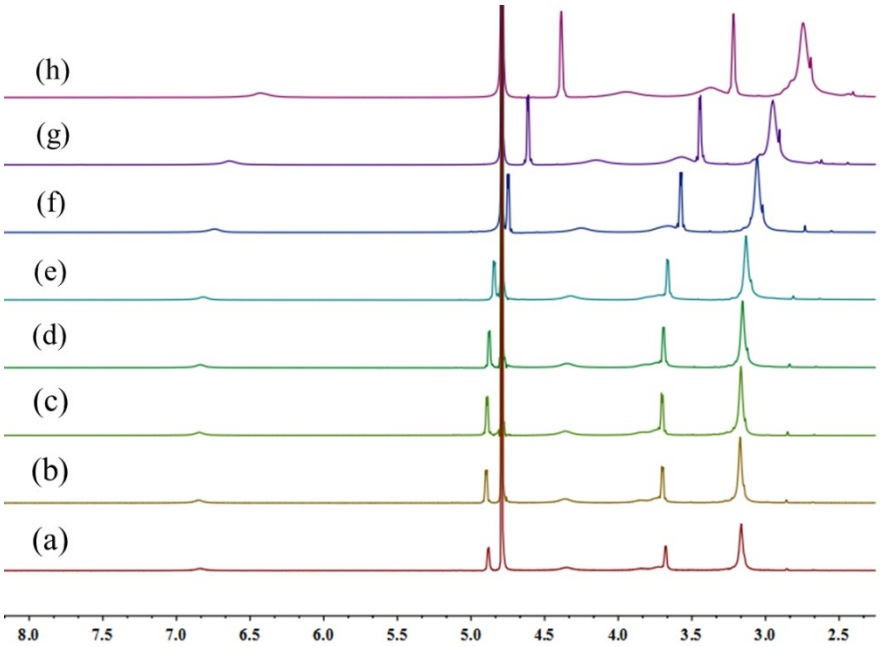

Fig. S20 Partial ^{1}H NMR spectra (400 MHz, D_2O, 25 °C) of **PT-2** at different concentrations: (a) 5.0 mg mL^{-1}; (b) 10 mg mL^{-1}; (c) 25 mg mL^{-1}; (d) 50 mg mL^{-1}; (e) 100 mg mL^{-1}; (f) 200 mg mL^{-1}; (g) 400 mg mL^{-1}; (h) 800 mg mL^{-1}.

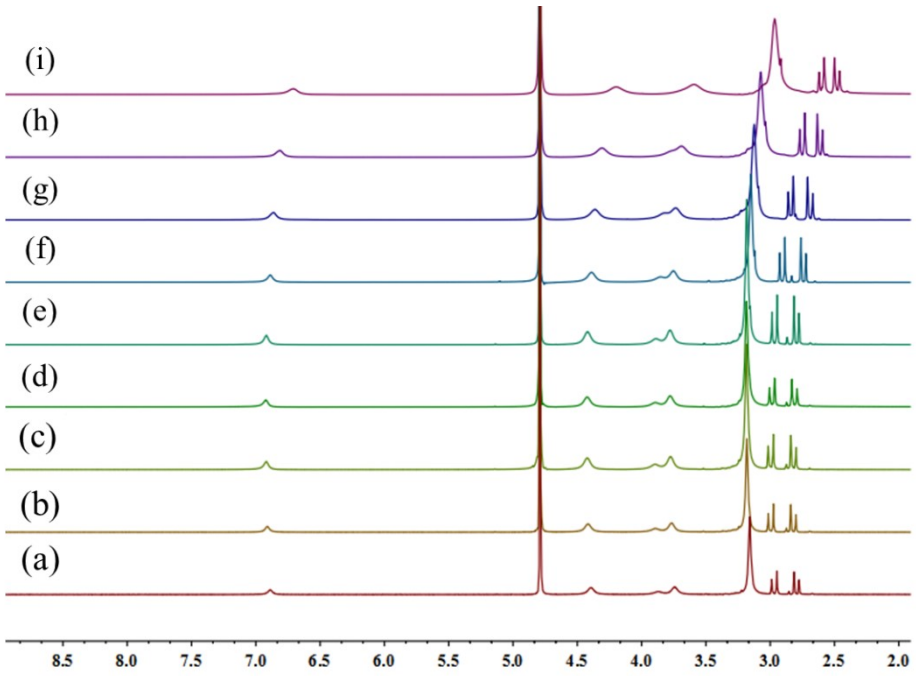

Fig. S21 Partial ^{1}H NMR spectra (400 MHz, D_2O, 25 °C) of **PC-1** at different concentrations: (a) 5.0 mg mL^{-1}; (b) 10 mg mL^{-1}; (c) 25 mg mL^{-1}; (d) 50 mg mL^{-1}; (e) 100 mg mL^{-1}; (f) 200 mg mL^{-1}; (g) 400 mg mL^{-1}; (h) 800 mg mL^{-1}; (i) 1600 mg mL^{-1}.

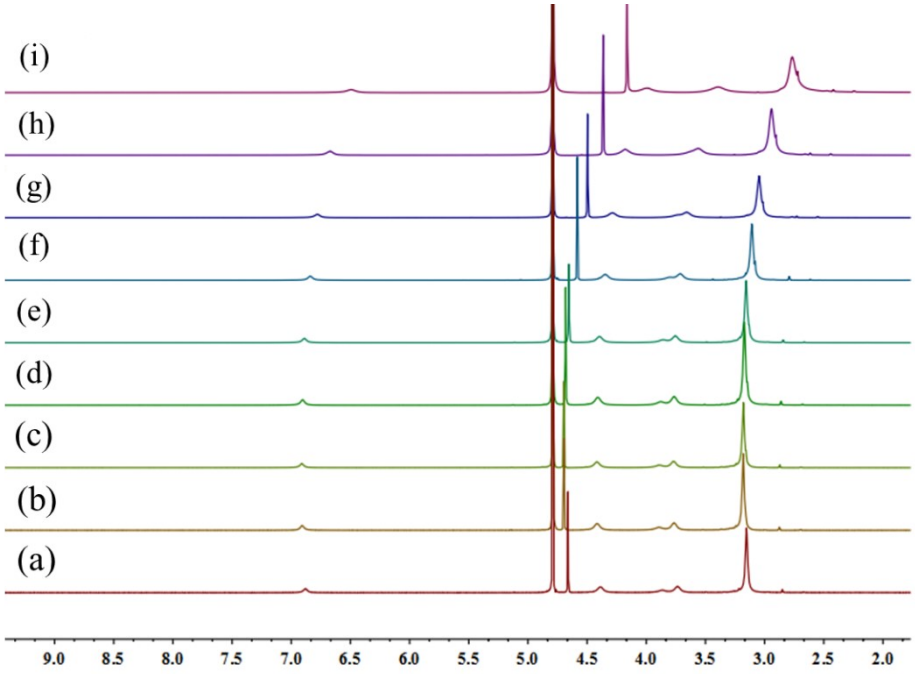

Fig. S22 Partial ^{1}H NMR spectra (400 MHz, D_2O, 25 °C) of **PD-2** at different concentrations: (a) 5.0 mg mL^{-1}; (b) 10 mg mL^{-1}; (c) 25 mg mL^{-1}; (d) 50 mg mL^{-1}; (e) 100 mg mL^{-1}; (f) 200 mg mL^{-1}; (g) 400 mg mL^{-1}; (h) 800 mg mL^{-1}; (i) 1600 mg mL^{-1}.

6. ^{1}H-^{1}H NOESY Spectra of Supramolecular Adhesives

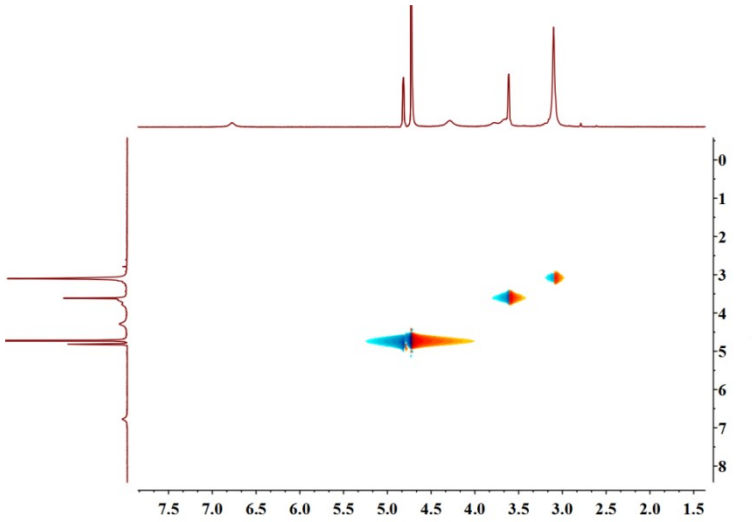

Fig. S23 Partial ^{1}H-^{1}H NOESY spectra (400 MHz, D_2O, 25 °C) of **PT-2** (5.0 mg mL^{-1}).

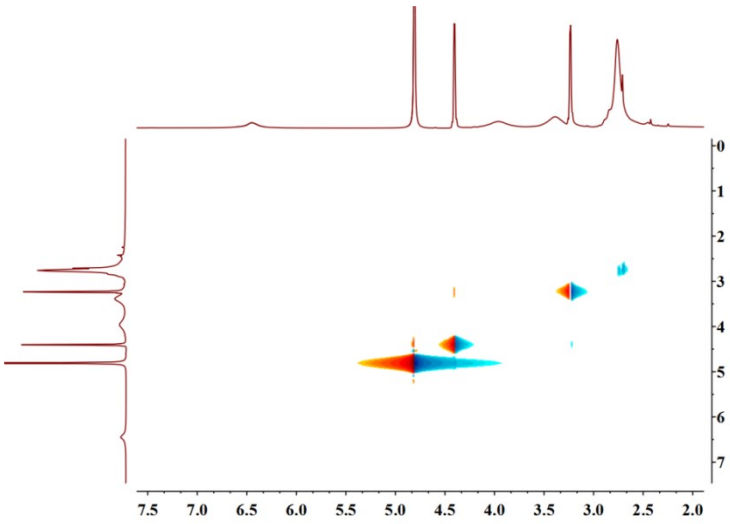

Fig. S24 Partial ^{1}H-^{1}H NOESY spectra (400 MHz, D_2O, 25 °C) of **PT-2** (800 mg mL^{-1}).

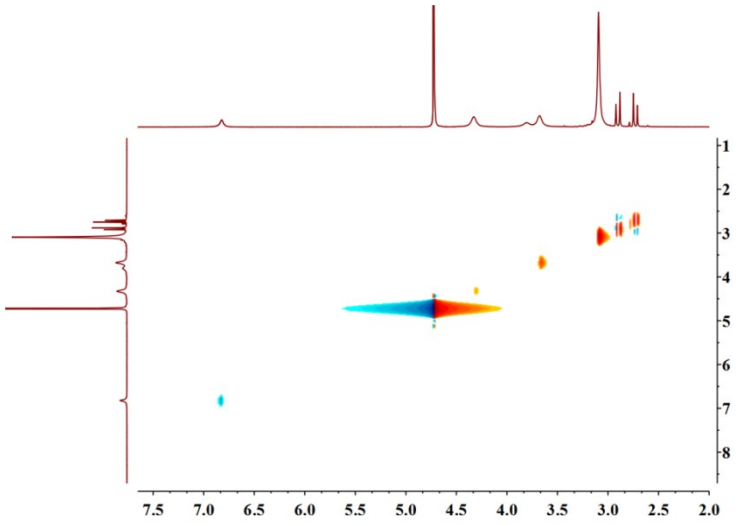

Fig. S25 Partial ^{1}H-^{1}H NOESY spectra (400 MHz, D_2O, 25 °C) of **PC-1** (5 mg mL^{-1}).

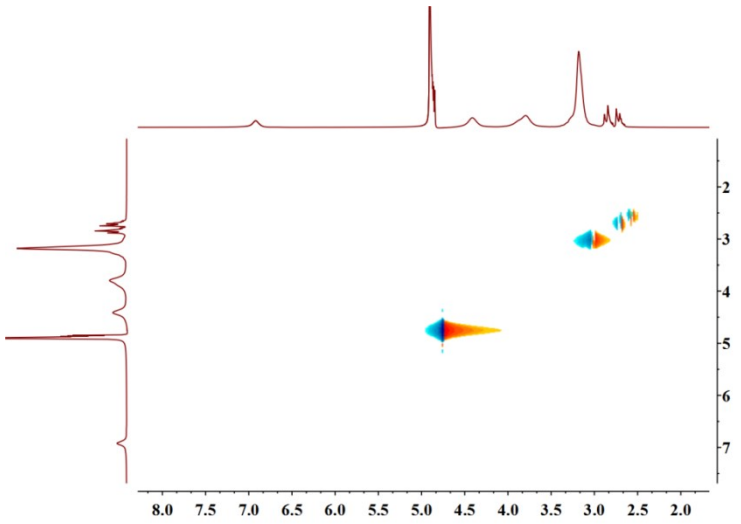

Fig. S26 Partial ^{1}H-^{1}H NOESY spectra (400 MHz, D_2O, 25 °C) of **PC-1** (800 mg mL^{-1}).

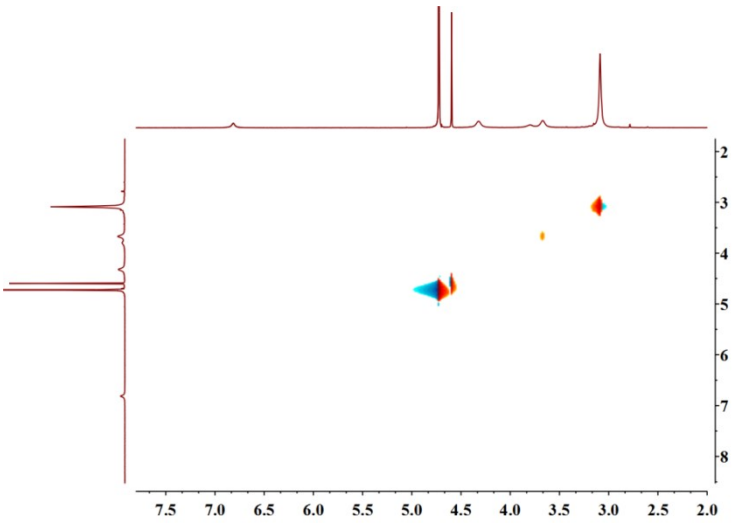

Fig. S27 Partial ^{1}H-^{1}H NOESY spectra (400 MHz, D_2O, 25 °C) of **PD-2** (5 mg mL^{-1}).

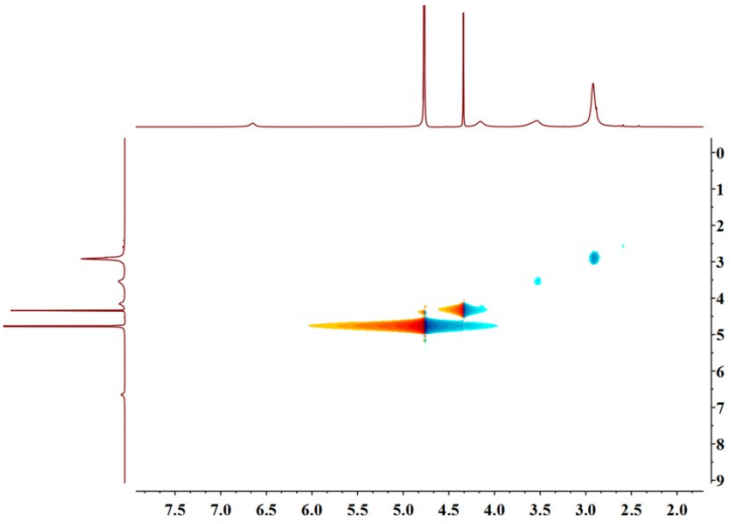

Fig. S28 Partial ^{1}H-^{1}H NOESY spectra (400 MHz, D_2O, 25 °C) of **PD-2** (800 mg mL^{-1}).

7. *Fourier-Transform IR (FT-IR) Spectra of Supramolecular Adhesives*

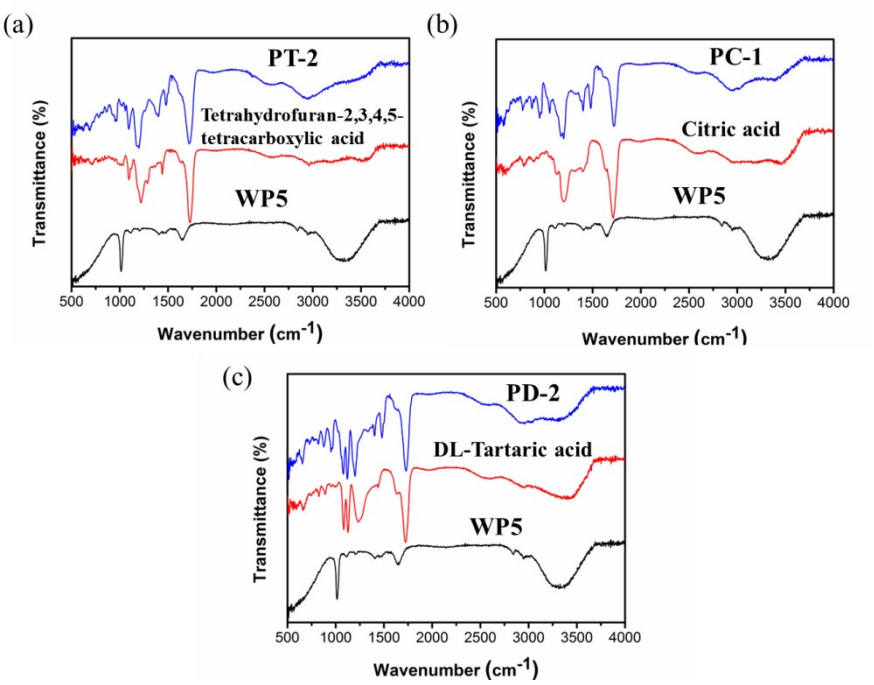

Fig. S29 FT-IR spectra of supramolecular adhesives, acids, and **WP5**: (a) **PT-2**, tetrahydrofuran-2,3,4,5-tetracarboxylic acid, **WP5**; (b) **PC-1**, citric acid, **WP5**; (c) **PD-2**, DL-tartaric acid, **WP5**.

8. *Scanning Electron Microscopy (SEM) of Supramolecular Adhesives*

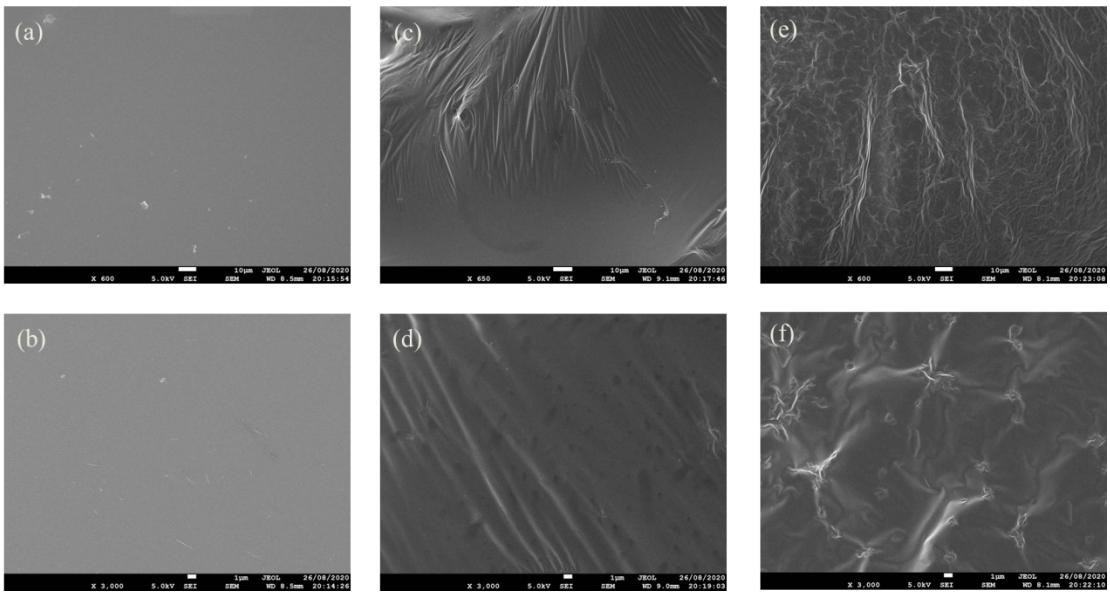

Fig. S30 SEM images of (a) and (b) **PT-2**; (c) and (d) **PC-1**; (e) and (f) **PD-2**.

9. Powder X-Ray Diffraction (PXRD) Pattern of Supramolecular Adhesives

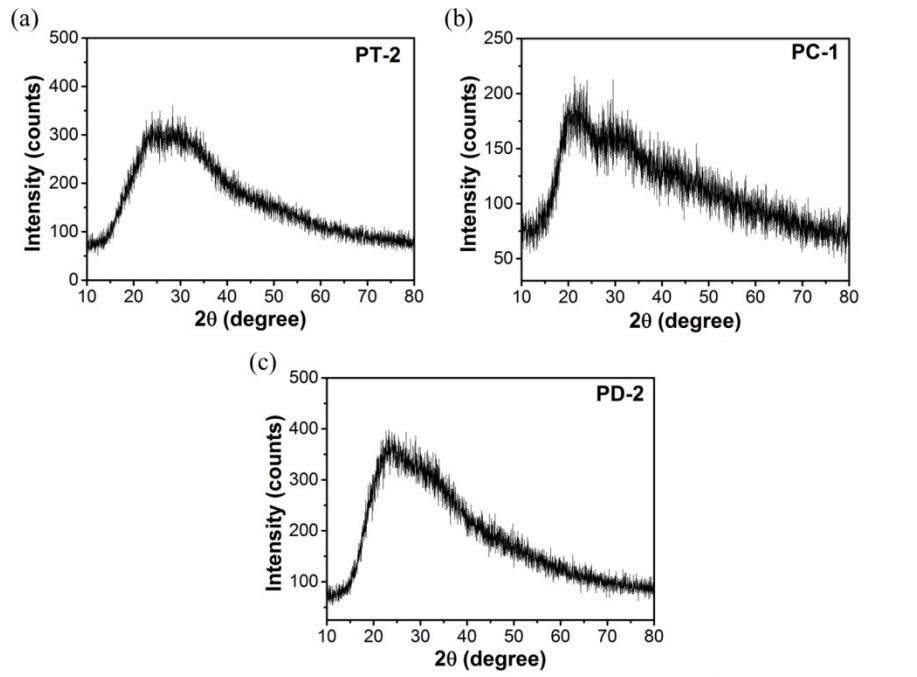

Fig. S31 PXRD spectra of supramolecular adhesives: (a) **PT-2**; (b) **PC-1**; (c) **PD-2**.

10. Differential Scanning Calorimeter (DSC) Measurements of Supramolecular Adhesives

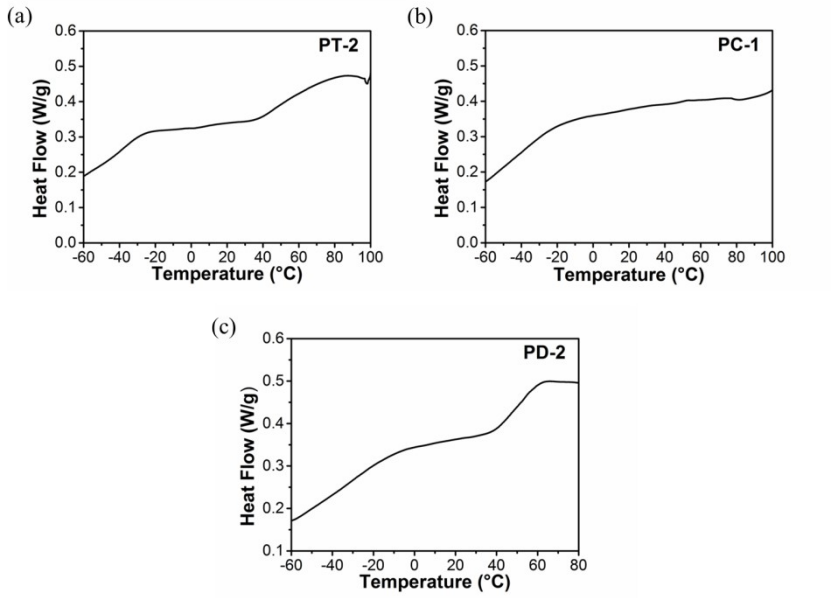

Fig. S32 DSC spectra of supramolecular adhesives: (a) **PT-2**; (b) **PC-1**; (c) **PD-2**.

11. *Thermogravimetric Analysis (TGA) of Supramolecular Adhesives*

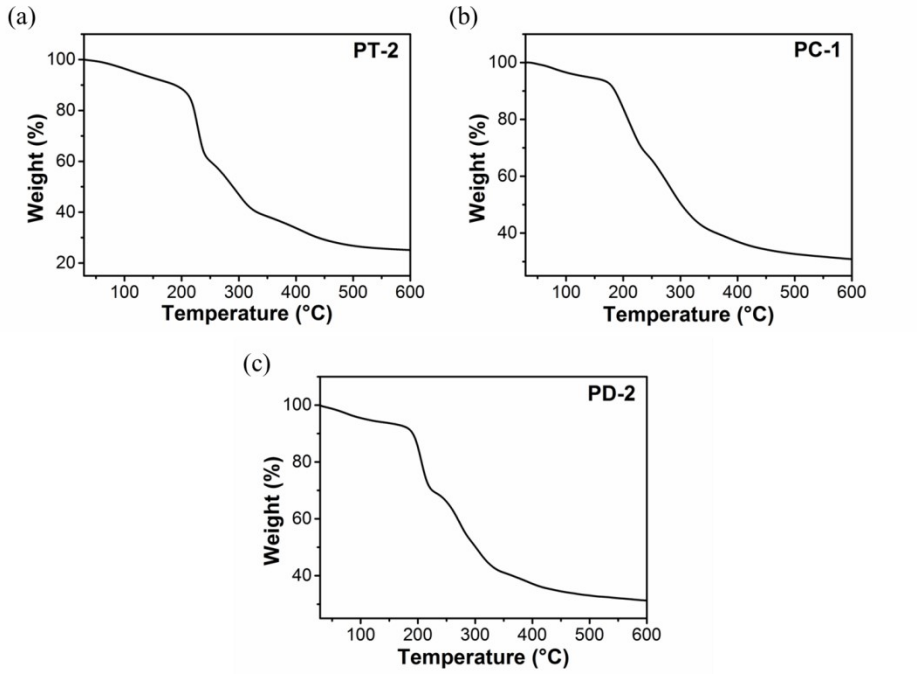

Fig. S33 TGA spectra of supramolecular adhesives: (a) **PT-2**; (b) **PC-1**; (c) **PD-2**.

12. *Rheology Measurements of Supramolecular Adhesives*

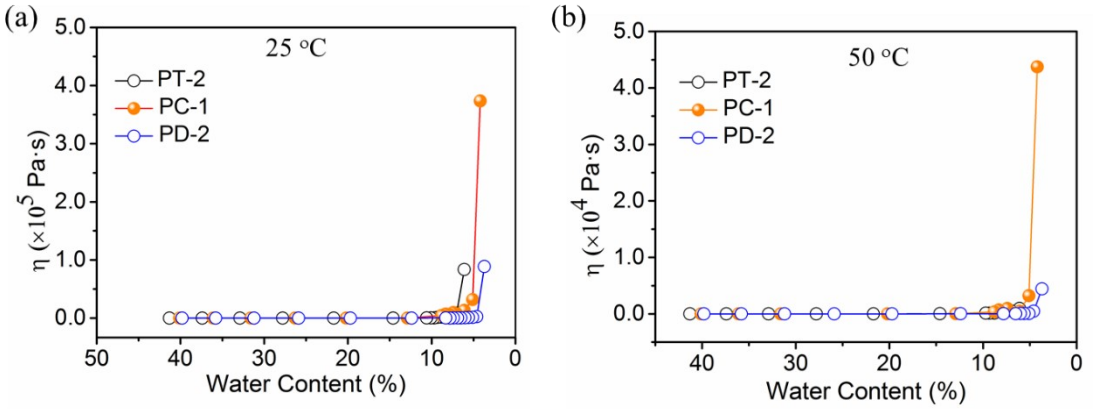

Fig. S34 Concentration-dependent composite viscosity (η) values of **WP5**-acid supramolecular adhesives on frequency sweep (angular frequency = 100 rad/s, shear strain = 1%,) at different temperature: (a) 25 °C; (b) 50 °C.

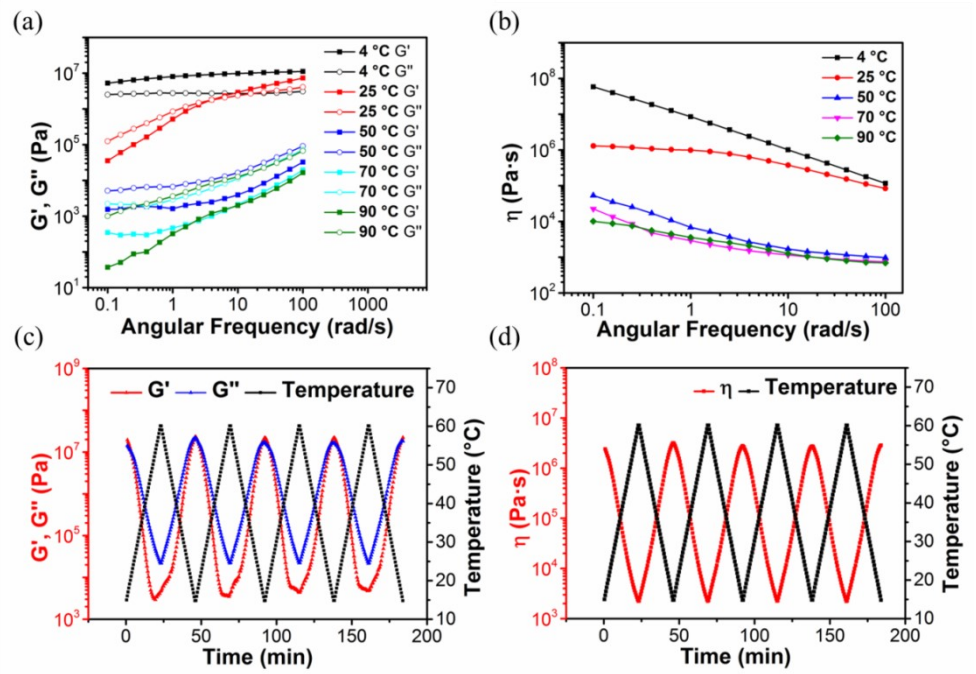

Fig. S35 (a) Storage modulus (G') and loss modulus (G'') values of **PT-2** on frequency sweep at different temperature; (b) composite viscosity (η) value of **PT-2** on frequency sweep at different temperature; (c) G' and G'' values of **PT-2** at reversible temperature-dependent rheological tests; (d) η value of **PT-2** at reversible temperature-dependent rheological tests.

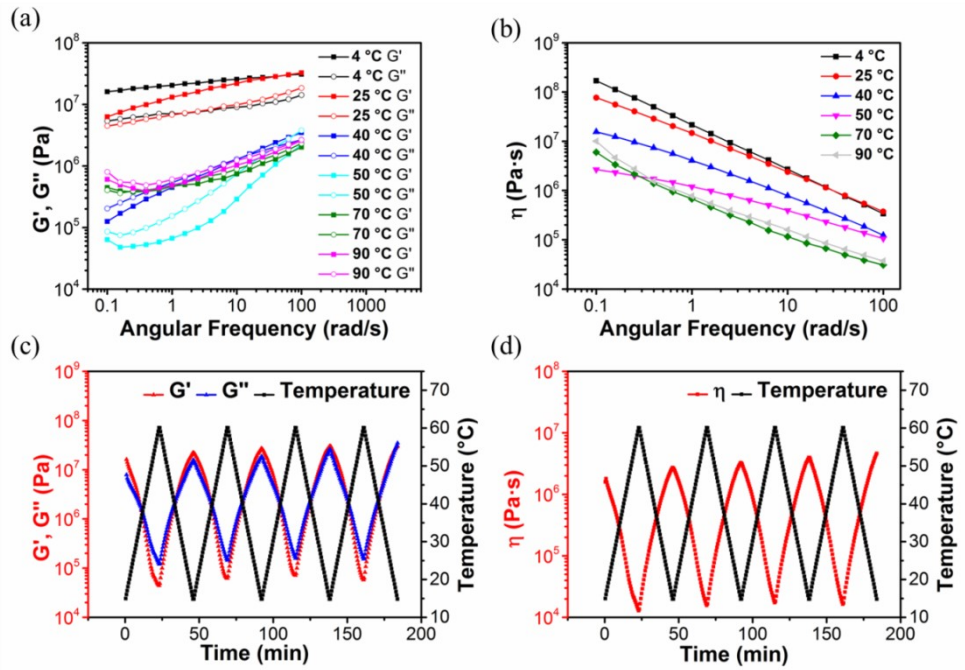

Fig. S36 (a) Storage modulus (G') and loss modulus (G'') values of **PC-1** on frequency sweep at different temperature; (b) composite viscosity (η) value of **PC-1** on frequency sweep at different temperature; (c) G' and G'' values of **PC-1** at reversible temperature-dependent rheological tests; (d) η value of **PC-1** at reversible temperature-dependent rheological tests.

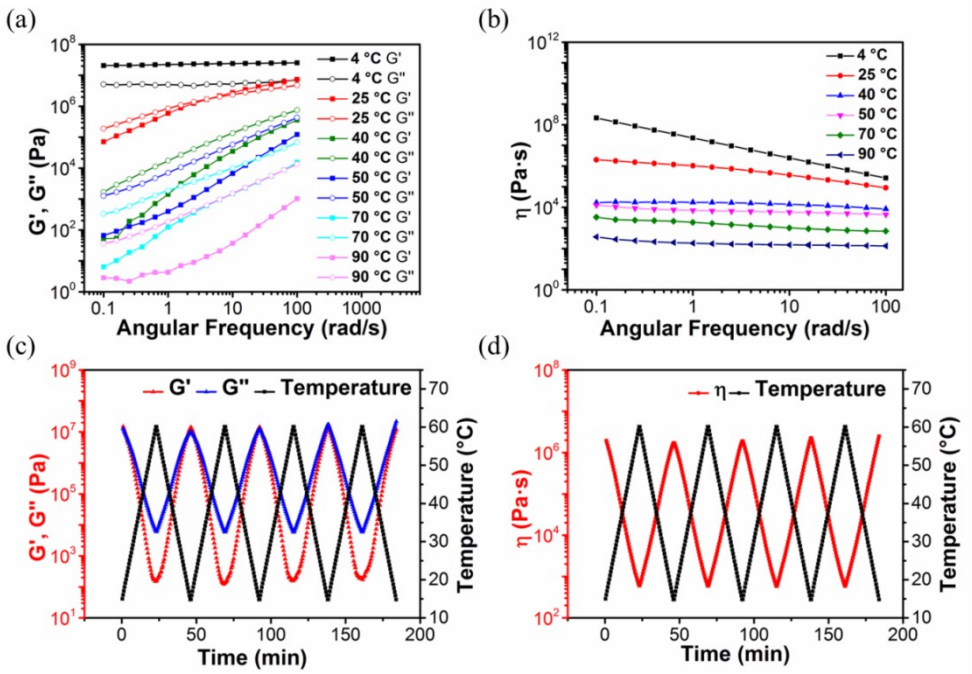

Fig. S37 (a) Storage modulus (G') and loss modulus (G'') values of **PD-2** on frequency sweep at different temperature; (b) composite viscosity (η) value of **PD-2** on frequency sweep at different temperature; (c) G' and G'' values of **PD-2** at reversible temperature-dependent rheological tests; (d) η value of **PD-2** at reversible temperature-dependent rheological tests.

13. Adhesion Measurements of Supramolecular Adhesives

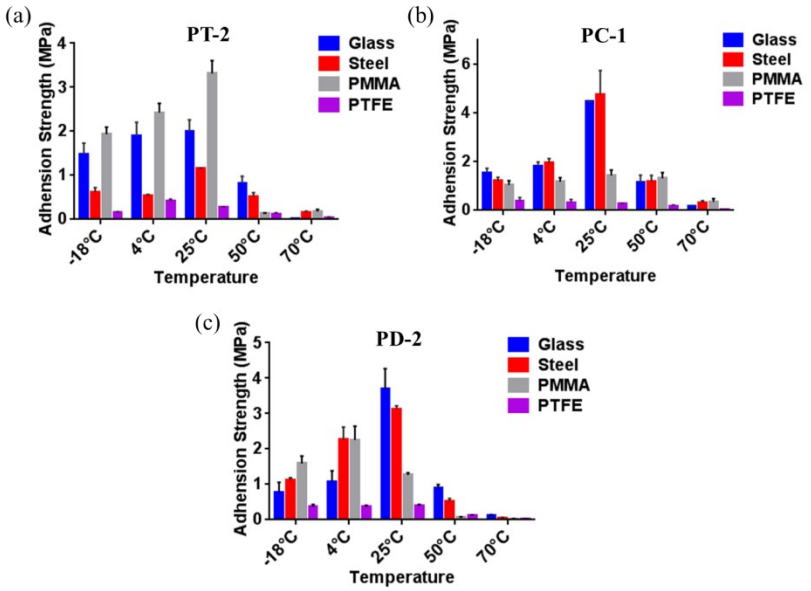

Fig. S38 Temperature-dependent adhesion strengths of supramolecular adhesives on different substrates (RH 44%): (a) **PT-2**; (b) **PC-1**; (c) **PD-2**.

Table S2. Adhesion strengths on glass of **PT-2**, **PC-1**, **PD-2** under different humidity and at 25 ºC for 3 h.

Adhesives	Adhesion strength (MPa)		
	24-29%	44%	84%
PT-2	0.99±0.10	1.99±0.27	1.16±0.27
PC-1	3.01±0.40	4.46±0.01	2.87±0.42
PD-2	2.96±0.56	3.69±0.58	3.54±0.45

14. Conductivity of Supramolecular Adhesives

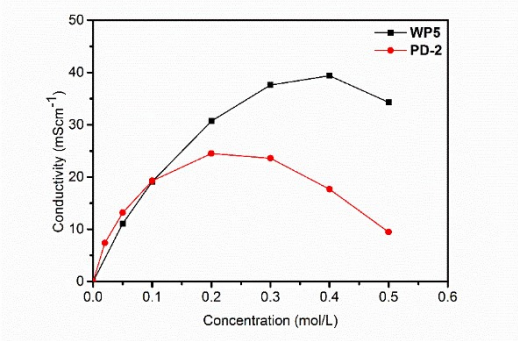

Fig. S39 Concentration-dependent conductivity of **WP5** and **PD-2** in aqueous solution at 25 °C.

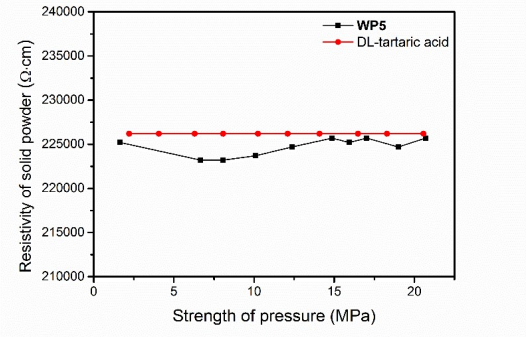

Fig. S40 The different solid-state resistivity at 0.1 μA of **WP5** and DL-tartaric acid at 25 °C.

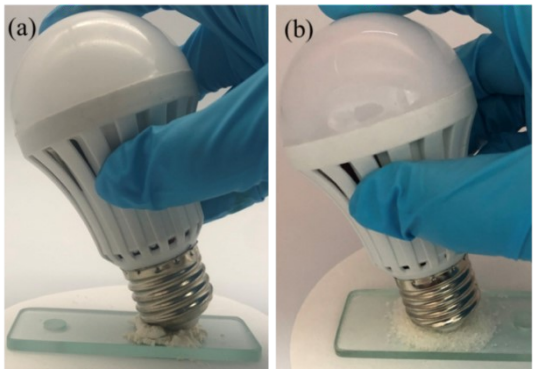

Fig. S41 The macroscopic conductivity: (a) the bulb is coated with **WP5** on the glass; (b) the bulb is coated with DL-tartaric acid on the glass.

15. DFT Calculation

All-electron DFT calculations have been carried out by the latest version of ORCA quantum chemistry software (Version 5.0.1). The BLYP functional was adopted for all calculations. For geometry optimization calculations, the def2SVP basis set was used. The DFT-D3 with BJ-damping was applied to correct the weak interaction to improve the calculation accuracy. Then, the interaction energy between adhesive and basis materials were calculated.[S5,S6]

Table S3. Interaction energy of compound 1 and compound 2 (molar ratio = 1:1), which used $(OH)_3SiOSi(OH)_2OSi(OH)_3$ as glass model.

Compound 1	**Compound 2**	***E* (Kcal/mol)**
Tetrahydrofuran-2,3,4,5-tetracarboxylic acid (**T**)	Tetrahydrofuran-2,3,4,5-tetracarboxylic acid (**T**)	-34.5
WP5	**WP5**	-109.3
WP5	Tetrahydrofuran-2,3,4,5-tetracarboxylic acid (**T**)	-64.4
WP5 : **T** (1:1)	$(OH)_3SiOSi(OH)_2OSi(OH)_3$	-74.7

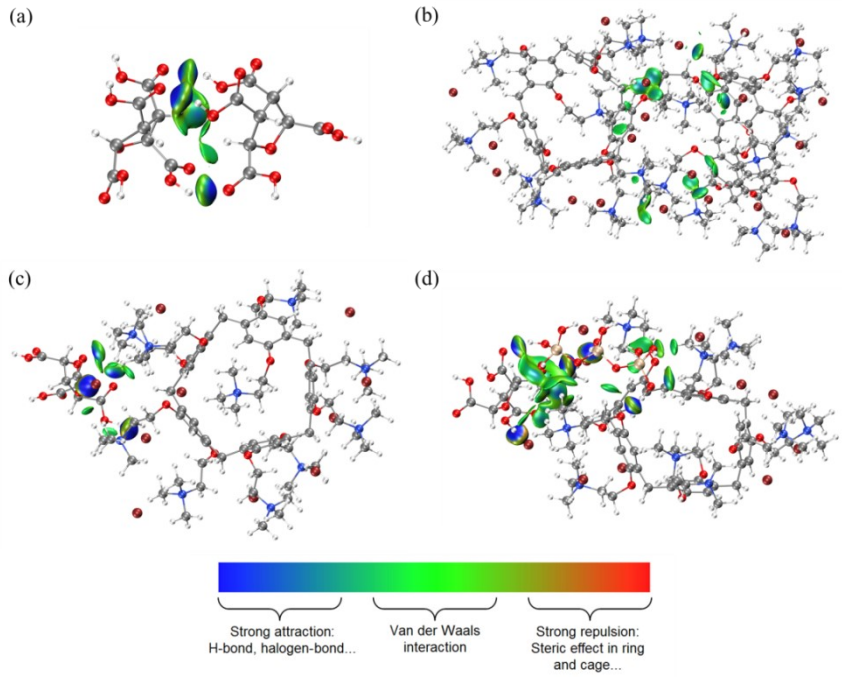

Fig. S42 The independent gradient model (IGM) isosurfaces of **WP5**-acid supramolecular adhesives. (a) IGM isosurfaces for the interaction between tetrahydrofuran-2,3,4,5-tetracarboxylic acid (**T**) and tetrahydrofuran-2,3,4,5-tetracarboxylic acid (**T**) (molar ratio 1:1); (b) IGM isosurfaces for the interaction between **WP5** and **WP5** (molar ratio 1:1); (c) IGM isosurfaces for the interaction between **WP5** and **T** (molar ratio 1:1); (d) IGM isosurfaces for the interaction between **WP5**, **T** and used $(OH)_3SiOSi(OH)_2OSi(OH)_3$ as glass model (molar ratio 1:1).

Molecular Dynamic Simulation

The interaction energy of the interface between pillar[5]arene-based supramolecular adhesive **PT-2** and hydrophilic substrates (glass and steel) was calculated by molecular dynamics to verify the adhesion mechanism of **PT-2** on hydrophilic substrates. According to our previous calculation method,[S7] we used Materials Studio software to carry out corresponding modeling and interface energy calculation. However, the molecular model was slightly different compared to before. the contact cell between **PT-2** and substrate surface with periodic structure was expanded to 43.4 × 43.4 $Å^2$. The thickness of glass was about 25.7 Å. The thickness of Steel was about 8.5 Å. Steel substrate contains 6 layers of Fe atoms. To equilibrate the model, a equilibrate process was followed under constant temperature and constant volume (NVT ensemble) at 298 K for 2000 ps. Then, the interaction energy between adhesive and basis materials were calculated by the following formula.

$$E_{interfacial} = E_{total} - (E_{adhesive} + E_{substrate})$$

$E_{interfacial}$: Interaction energy between supramolecular adhesive materials and substrate, and minus means adsorption.

E_{total}: The total potential energy of adhesive-substrate system.

$E_{adhesive}$: The potential energy of adhesive.

$E_{substrate}$: The potential energy of substrate.

Table S4. Interaction energy between **PT-2** and hydrophilic substrates.

Substrate	*E* (Kcal/mol)			
	E_{total}	$E_{adhesive}$	$E_{substrate}$	$E_{interfacial}$
Glass	-67506.1	-13043.4	-52813.4	-1649.3
Steel	-128911.8	-13419.0	-112915.5	-2577.3

16. Supplementary Videos

Video S1. Macroscopic adhesion behaviour of **PC-1**.

Video S2. Fiber drawing of **PD-2**.

Video S3. Macroscopic adhesion behaviour of **PC-1** in dichloromethane.

17. References

S1. Y. J. Ma, X. F. Ji, F. Xiang, X. D. Chi, C. Y. Han, J. M. He, Z. Abliz, W. X. Chen and F. H. Huang, *Chem. Commun.*, 2011, **47**, 12340–12342.

S2. B. Hua, L. Shao, G. C. Yu and F. H. Huang, *Chem. Commun.*, 2016, **52**, 10016–10019.

S3. S. Y. Dong, J. Leng, Y. X. Feng, M. Liu, C. J. Stackhouse, A. Schönhals, L. Chiappisi, L. Y. Gao, W. Chen, J. Shang, L. Jin, Z. H. Qi and C. A. Schalley, *Sci. Adv.*, 2017, **3**, eaao0900.

S4. S. G. Wu, C. Y. Cai, F. F. Li, Z. J. Tan and S. Y. Dong, *Angew. Chem., Int. Ed.*, 2020, **59**, 11871–11875.

S5. F. Weigend and R. Ahlrichs, *Phy. Chem. Chem. Phys.*, 2005, **7**, 3297–3305.

S6. S. Grimme, S. Ehrlich and L. Goerigk, *J. Comput. Chem.*, 2011, **32**, 1456–1465.

S7. X. Li, Y. Deng, J. L. Lai, G. Zhao and S. Y. Dong, *J. Am. Chem. Soc.*, 2020, **142**, 5371–5379.